

Unraveling the effect of silent, intronic and missense mutations on VWF splicing: contribution of next generation sequencing in the study of mRNA

Nina Borràs,^{1,2} Gerard Orriols,¹ Javier Batlle,³ Almudena Pérez-Rodríguez,³ Teresa Fidalgo,⁴ Patricia Martinho,⁴ María Fernanda López-Fernández,³ Ángela Rodríguez-Trillo,³ Esther Lourés,³ Rafael Parra,^{1,2} Carme Altisent,² Ana Rosa Cid,⁵ Santiago Bonanad,⁵ Noelia Cabrera,⁵ Andrés Moret,⁵ María Eva Mingot-Castellano,⁶ Nira Navarro,⁷ Rocío Pérez-Montes,⁸ Sally Marcellin,⁹ Ana Moreto,¹⁰ Sonia Herrero,¹¹ Inmaculada Soto,¹² Núria Fernández-Mosteirín,¹³ Víctor Jiménez-Yuste,¹⁴ Nieves Alonso,¹⁵ Aurora de Andrés-Jacob,¹⁶ Emilia Fontanes,¹⁷ Rosa Campos,¹⁸ María José Paloma,¹⁹ Nuria Bermejo,²⁰ Ruben Berruero,²¹ José Mateo,²² Karmele Arribalzaga,²³ Pascual Marco,²⁴ Ángeles Palomo,²⁵ Nerea Castro Quismondo,²⁶ Belén Iñigo,²⁷ María del Mar Nieto,²⁸ Rosa Vidal,²⁹ María Paz Martínez,³⁰ Reyes Aguinaco,³¹ Jesús María Tenorio,³³ María Ferreiro,³³ Javier García-Frade,³⁴ Ana María Rodríguez-Huerta,³⁵ Jorge Cuesta,³⁶ Ramón Rodríguez-González,³⁷ Faustino García-Candel,³⁸ Manuela Dobón,³⁹ Carlos Aguilar,⁴⁰ Francisco Vidal^{1,2,41} and Irene Corrales^{1,2}

¹Banc de Sang i Teixits, Barcelona, Spain; ²Institut de Recerca Vall d'Hebron - Universitat Autònoma de Barcelona (VHIR-UAB), Spain; ³Complejo Hospitalario Universitario A Coruña, INIBIC, Spain; ⁴Centro Hospitalar e Universitário de Coimbra, Portugal; ⁵Hospital Universitario y Politécnico La Fe, Valencia, Spain; ⁶Hospital Regional Universitario de Málaga, Spain; ⁷Hospital Universitario Dr. Negrín, Las Palmas de Gran Canaria, Spain; ⁸Hospital Universitario Marqués de Valdecilla, Santander, Spain; ⁹Salud Castilla y León, Segovia, Spain; ¹⁰Hospital Universitario Cruces, Barakaldo, Spain; ¹¹Hospital Universitario de Guadalajara, Spain; ¹²Hospital Universitario Central de Asturias, Oviedo, Spain; ¹³Hospital Universitario Miguel Servet, Zaragoza, Spain; ¹⁴Hospital Universitario La Paz, Madrid, Spain; ¹⁵Hospital Infanta Cristina, Badajoz, Spain; ¹⁶Complejo Hospitalario Universitario Santiago de Compostela, Spain; ¹⁷Hospital Universitario Lucus Augusti, Lugo, Spain; ¹⁸Hospital Jerez de la Frontera, Cádiz, Spain; ¹⁹Hospital Virgen del Camino, Pamplona, Spain; ²⁰Hospital San Pedro de Alcántara, Cáceres, Spain; ²¹Hospital Sant Joan de Deu, Barcelona, Spain; ²²Hospital Sta Creu i St Pau, Barcelona, Spain; ²³Hospital Universitario Fundación de Alcorcón, Madrid, Spain; ²⁴Hospital General de Alicante, Spain; ²⁵Hospital Regional Universitario Carlos Haya, Málaga, Spain; ²⁶Hospital Universitario 12 de Octubre, Madrid, Spain; ²⁷Hospital Clínico San Carlos, Madrid, Spain; ²⁸Complejo Hospitalario de Jaén, Spain; ²⁹Fundación Jiménez Díaz, Madrid, Spain; ³⁰Hospital Nuestra Sra. de Sonsoles de Ávila, Spain; ³²Hospital Joan XXIII, Tarragona, Spain; ³²Hospital Ramón y Cajal, Madrid, Spain; ³³Hospital Montecelo, Pontevedra, Spain; ³⁴Hospital Río Hortega, Valladolid, Spain; ³⁵Hospital Gregorio Marañón, Madrid, Spain; ³⁶Hospital Virgen de la Salud, Toledo, Spain; ³⁷Hospital Severo Ochoa, Madrid, Spain; ³⁸Hospital Universitario Virgen Arrixaca, Murcia, Spain; ³⁹Hospital Lozano Blesa, Zaragoza, Spain; ⁴⁰Hospital Santa Bárbara, Soria, Spain and ⁴¹CIBER de Enfermedades Cardiovasculares, Madrid, Spain

©2019 Ferrata Storti Foundation. This is an open-access paper. doi:10.3324/haematol.2018.203166

Received: August 3, 2018.

Accepted: October 19, 2018.

Pre-published: October 25, 2018.

Correspondence: IRENE CORRALES

icorrales@bst.cat/fvidal@bst.cat

SUPPLEMENTARY DATA

SUPPLEMENTARY METHODS

VWF mRNA amplification

The primers used have been reported previously,¹ except for those specifically designed to analyze certain mutations (Online Supplementary Table S1). The PCR mix contained 1X PCR Buffer, 1.5 mM MgCl₂, 200 μM dNTPs, 2 U Platinum Taq DNA polymerase, 0.75 μM of each primer, and cDNA in a total volume of 25 μL. After initial denaturation at 94°C for 3 min, 38 cycles of 94°C for 20 sec, 62°C for 30 sec, and 72°C for 1 min were performed, followed by a final extension at 72°C for 3 min.

CLC Bio Data analysis parameters

Primer sequences and low-quality regions were trimmed and aligned against the WT VWF mRNA sequence with specific parameter settings. The Basic Variant Detection algorithm was applied for single nucleotide variant-calling and the Indels and Structural Variants tool was performed to identify insertions and deletions produced by alternative splicing due to mutations. Analytical settings of both algorithms are described in Online Supplementary Figure S1.

Finally, a specific probe was designed to each pre-characterized aberrant transcript and used to perform a second alignment from the original dataset. The results indicate the number of reads that aligned to each mRNA probe.

Intron retention of exon 25

To determine whether intron 25 was retained within the mature mRNA of patient UMP09, RT-PCR reactions using 2 allele-specific primer combinations were performed. In the first primer pair, the forward was designed at the junction of exon 24-25 (VWFR24/25-1) and the reverse primer was designed inside intron 25 (VWF_E25-2). In the second primer pair, the forward primer targeted intron 25 (VWF_E26-1) and the reverse was located across the junction of exon 26-27 (VWFR26/27-2).

Intron retention of exon 45

To determine whether intron 45 was retained within the mature mRNA of patients UMP05 and UMP06, RT-PCR reactions using 2 allele-specific primers combinations were performed. In the first primer pair, the forward was designed at the junction of exon 44-45 (VWFR44/45-1C) and the reverse primer was designed inside intron 45 (VWF_E45-2). In the second primer pair, the

forward primer targeted intron 45 (VWF_E46-1) and the reverse was located across the junction of exon 47-48 (VWFR46/47-2).

X-chromosome inactivation

The X-chromosome inactivation profile studies were performed on DNA extracted from peripheral blood. The study was done using HpaII digestion. Genomic DNA samples were digested with the methylation-sensitive enzyme HpaII (Invitrogen) and subjected to PCR amplification of the highly polymorphic CAG repeat sequence in the first exon of the human androgen receptor gene (HUMARA), with specific fluorescent primers. The primer sequences are shown in Online Supplementary Table S1. The PCR products, both before and after HpaII digestion, were electrophoresed on an automated DNA sequencer (ABI 3130XL; Applied Biosystems, Warrington, United Kingdom) and analyzed by GeneMapper software (Applied Biosystems).²

SUPPLEMENTARY TABLES

Table S1. Specific primers used for amplification and sequencing by Sanger of VWF RNA.

Forward Primer	Location	Reverse Primer	Location	Purpose	Product size
VWRNA1-1 CTACATAACAGCAAGACAGTCC	Exon 1	VWRNA1-2 GGTGCTCTTCAGAAGCTGG	Exon 7	Full-length VWF amplification	836 bp
VWRNA2-1 GCAGTCCATGCAACATCTCC	Exon 6	VWRNA2-2 CCTTGTGAAACTGAAGCATGG	Exon 12	Full-length VWF amplification	762 bp
VWRNA3-1 CCATTGTCATTGAGACTGTCCAC	Exon 11	VWRNA3-2 CCTGACCTGCCGCTCTCT	Exon 16	Full-length VWF amplification	744 bp
VWRNA4-1 GCGTGGCGGAGCCAGG	Exon 15	VWRNA4-2 GTAAACCTGGGACCTTTCG	Exon 21	Full-length VWF amplification	796 bp
VWRNA5-1 CATGGCCCACTACCTCACC	Exon 20	VWRNA5-2 GGTGGTGACCTGGAGGAC	Exon 25	Full-length VWF amplification	752 bp
VWRNA6-1 TCCTGTGAGTCCATTGGGG	Exon 25	VWRNA6-2 GGAAGCGACCGTCAGAGC	Exon 28	Full-length VWF amplification	750 bp
VWRNA7-1 CTTTGTGGTGGACATGATGG	Exon 28	VWRNA7-2 CCTCTCTGACCACAGCTTC	Exon 28	Full-length VWF amplification	876 bp
VWRNA8-1 CCTGCAGCGGGTGCAGG	Exon 28	VWRNA8-2 CCTGGTCACGGACGTCTC	Exon 31	Full-length VWF amplification	728 bp
VWRNA9-1 AAATCGGGGATGCCCTGGG	Exon 30	VWRNA9-2 GGAGGTGACGGTGAATGGG	Exon 35	Full-length VWF amplification	772 bp
VWRNA10-1 GGAGGTGATTCTCCATAATGG	Exon 35	VWRNA10-2 CTGCGTTGTGCAGTTGACC	Exon 39	Full-length VWF amplification	930 bp
VWRNA11-1 GTGAGCATGGCTGTCCCC	Exon 38	VWRNA11-2 GGATGCCGTGATGGCCCT	Exon 43	Full-length VWF amplification	753 bp
VWRNA12-1 GTGTGTCCACCGAAGCACC	Exon 43	VWRNA12-2 CCCTTTGATGAACACAAGTGT	Exon 49	Full-length VWF amplification	813 bp
VWRNA13-1 CGTGATGAGACGCTCCAGG	Exon 49	VWRNA13-2 CCTCTGCATGTTCTGCTCT	Exon 52	Full-length VWF amplification	546 bp
VWRNA3-1 CCATTGTCATTGAGACTGTCCA	Exon 11	VWRNA_E15-2 CGTCGTAGCGGCAGTTCC	Exon 15	primers to avoid alternative splicing in leukocytes	564 bp
VWFR4-1 GCCTCTCCGTGTATCTTGG	Exon 4	VWRNA1-2B GGTGCTCTTCAGAAGCTGG	Exon 7	Exon 5-6	446 bp
VWF22-1 GGTCCTGAAGCAGACATAACC	Exon 22	VWF26-2A CTCCCGGAGATTCTCTCC	Exon 26	Exon 25 complete	466 bp
VWFR24/25-1 GACTGCAACAAGCTGGTGG	Junction exon 24-25	VWF_E25-2 ATCCAGTCCCTACTAACAACCT	Intron 25	Intron 25 retention	301 bp
VWF_E26-1 ACATAGCAAGACCCCATCTG	Intron 25	VWFR26/27-2 CATCCAGGATTTCCCTGG	Junction exon 26-27	Intron 25 retention	401 bp
VWFR43/44-1 GGACAGCTGTCGGTCGGG	Junction exon 43-44	VWF_E45-2 CAGGAGCCAAAAGTGGAAAG	Intron 45	Intron 45 retention	381 bp
VWF_E46-1 CGACCGATACAGGAGGGAG	Intron 45	VWF47/48-2 ATTTTCTTCTGTAACCCAGG	Junction exon 47-48	Intron 45 retention	295 bp
VWFR41/42-1 CCCAACTCACCTGCGCC	Junction exon 41-42	VWFR44/45-2 TGGGAGCCGACACTCTTCC	Junction exon 44-45	Exon 43 complete	494 bp

At the top of the table, primers previously designed by Corrales et al.¹ At the bottom of the table, primers newly designed to analyze potential splice site mutations included in this study.

Table S2. Additional laboratory and clinical data of VWD patients

Patients code	VWD	Hospital	Registry code	Age	Sex	ABO	Multimeric pattern	BS	Family history
UMP01	3 carrier	CHUC	P64's mother	37	F	A	ND	0	Yes
UMP02	1H	CHUAC	C01P034F17	32	M	O+	NORMAL	2	Yes
UMP03	1	CHUAC	C01P080	40	M	O+	ND	1	NA
UMP04	1	HUVH	-	38	F	O+	ND	C, D	No
UMP05	1	CHUAC	C01P006F03	39	F	O+	NORMAL	11	No
UMP06	2A/2M	CHUAC	C01P024F12	33	F	O	SMEAR	10	No
UMP07	1	HUVH	-	47	M	O+	ND	B	Yes
UMP08	1	HUVH	-	42	M	O+	ND	B	Yes
UMP09	1	HUVH	-	20	F	ND	ND	B, C	Yes
UMP10	3 carrier	HUVH	-	45	F	O	ND	A, C, E	Yes
UMP11	1	CHUAC	C01P051F11	36	M	O+	NORMAL	7	Yes
UMP12	3	HUVH	C03P021F25	15	M	A	ND	10	Yes
UMP13	2A	HUVH	C03P048F231	15	F	O+	↓HMWM	0	Yes
UMP14	1	CHUC	P12	10	M	ND	ND	16	Yes
UMP15	3	HUVH	-	25	F	O	ND	B, E	Yes

The subtype 1H (historical) refers to patients previously diagnosed as type 1 VWD that, at the time of enrollment at the PCM-EVW-ES project, show a slight decrease or even a normal VWF plasma levels. Bleeding scores calculated with the International Society on Thrombosis and Haemostasis bleeding assessment tools (ISTH-BAT) were used to assess bleeding in patients included in the Spanish (PCM-EVW-ES) and Portuguese registries. In the remaining patients, symptoms were assigned letters: A, easy bruising; B, epistaxis; C, prolonged bleeding from wounds; D, menorrhagia; and E, postoperative bleeding. BS indicates bleeding score; CHUAC, Complejo Hospitalario Universitario A Coruña, Spain; CHUC, Centro Hospitalar e Universitário de Coimbra, Portugal; F, female; HUVH, Hospital Universitari Vall d'Hebron, Barcelona, Spain; HMWM, high molecular weight multimers; M, male; NA; not available; ND, not determined and; VWD, von Willebrand disease.

Table S3. Summary of the *in silico* analysis of PSSM

Mutation Type	NT change	AA change	Exon	Intron	Affected splice site	Adjacent nucleotides	NetGene2		Neural Network Splice		MaxEnt		HSF		Score	HSF Interpretation
							wt	var	wt	var	wt	var	wt	var		
Intronic	c.1533+1G>A	-	-	13	DSS intron 13	GAAgtaggt>GAAgtaggt	1	Native DSS destroyed	0.98	Native DSS destroyed	10.29	2.1	90.71	63.87	4/4	Alteration of the WT donor site, most probably affecting splicing.
	c.3379+1G>A	-	-	25	DSS intron 25	TGCgtgag>TGCCatgag	0.95	Native DSS destroyed	0.90	Native DSS destroyed	8.56	0.38	81.32	54.48	4/4	Alteration of the WT donor site, most probably affecting splicing.
	c.5664+2T>C	-	-	33	DSS intron 33	AGGgtaagt>AGGgcaagt	0.83	Native DSS destroyed	1	Native DSS destroyed	10.45	2.7	94.19	67.35	4/4	Alteration of the WT donor site, most probably affecting splicing.
	c.7081+6G>T	-	-	41	DSS intron 41	taaggcctc>taagtctct	1	1	1	1	9.63	11.37	91.56	93.49	0/4	No significant splicing motif alteration detected.
	c.7082-2A>G	-	-	41	ASS intron 41	cctcagCCT>cctcggCCT	NP	Native ASS destroyed	0.69	Native ASS destroyed	6.68	-1.27	88.28	59.34	4/4	Alteration of the WT donor site, most probably affecting splicing.
	c.7730-4C>G	-	-	45	ASS intron 45	tccccagA>tccccagA	1	1	0.99	0.99	11.71	13.00	91.73	91.11	0/4	Activation of an intronic cryptic acceptor site. Potential alteration of splicing.
	c.7730-56C>T	-	-	45	ASS intron 45	tcgccgtc>tcgctggtc	1	1	0.99	0.99	6.54	7.02	87.43	88.69	0/4	Creation of an intronic ESE site. Probably no impact on splicing.
	c.8155+3G>C	-	-	50	DSS intron 50	ATgtgagt>ATgtcagt	0.54	Native DSS destroyed	0.94	Native DSS destroyed	7.83	2.02	85.46	78.65	3/4	Alteration of the WT donor site, most probably affecting splicing.
	c.8254-5T>G	-	-	51	ASS intron 51	ttcttcag>ttctggcag	1	0.96	0.99	0.94	12.47	10.09	92.5	88.8	0/4	No significant splicing motif alteration detected.
Synonymous	c.546G>A	p.Ser182	6	-	New ASS	CCTCGGACC>CCTCAGACC	0.71	0.33	0.90	0.88	NP	NP	57.31	86.26	2/4	Activation of an exonic cryptic acceptor site, with presence of one or more cryptic branch point(s). Potential alteration of splicing.
	c.3291C>T	p.Cys1097	25	-	New DSS	ACTGCGCCT>ACTGTGCCT	0.95	0.95	0.90	0.90	NP	NP	NP	NP	0/4	Creation of an exonic ESS site. Potential alteration of splicing.
	c.3426T>C	p.Cys1142	26	-	Alteration GT	AGTGTGAGT>AGTGCAGT	0.67	0.67	1	1	6.96	-0.79	82.16	55.33	2/4	Alteration of an exonic ESE site. Potential alteration of splicing.
	c.4866C>T	p.Asp1622	28	-	Not affected	GAGACATCC>GAGATATCC	0.96	0.96	0.97	0.97	NP	NP	75.04	75.88	0/4	Alteration of an exonic ESE site. Potential alteration of splicing.
	c.7437G>A	p.Ser2479	43	-	DSS intron 43	GGTCGgtgag>GGTCAGtgag	1	0.95	0.98	0.63	3.52	11.11	92.11	81.53	3/4	Alteration of the WT donor site, most probably affecting splicing.
Missense	c.449T>C	p.Leu150Pro	5	-	Not affected	CTGCTGTCA>CTGCCGTCA	1	1	0.98	0.98	NP	NP	85.99	86.64	0/4	No significant splicing motif alteration detected.
	c.1109G>A	p.Cys370Tyr	9	-	DSS intron 9	ACCTGgtaa>ACCTAgtaa	NP	NP	0.31	Native DSS destroyed	5.67	-2.74	81.00	70.42	3/4	Alteration of the WT donor site, most probably affecting splicing.
DelIns	c.3485_3486delInsTG	p.Pro1162Leu	26	-	Not affected	GAGCCACTGG>GAGCTGCTGG	0.67	0.83	1	1	6.69	7.09	71.11	71.95	1/4	Creation of an exonic ESS site. Potential alteration of splicing.
	c.3223-7_3236dup	p.Pro1079_Tyr1080InsLeu uGlnValAspProGluPro	25	-	New ASS	cagG----- TGGA>cagGtttcagGTGGA	0.95	0,95 + New ASS (0.81)	0.73	0,59 + New ASS	3.09	4.86	15.42	84.46	4/4	Activation of an exonic cryptic acceptor site. Potential alteration of splicing.
	c.6699_6702dup	p.Cys2235Argfs*8	38	-	Not affected	AGGC----TGTT>AGGCAGGCTGTT	0,93	0,93	0,97	0,98	4,3	4,27	82,59	83,23	0/4	Alteration of an exonic ESE site. Potential alteration of splicing.

The *in silico* global score is based on the number of *in silico* algorithms that predicted a splicing effect. *In silico* analysis of mutations included in the PCM-ES-EVW registry was performed by ALAMUT. *In silico* analysis of the mutations not included in the PCM-EVW-ES registry was performed individually under the established parameters of each algorithm, as well as NetGene2 (unavailable in ALAMUT). For HSF and MaxEnt, the sequence analyzed is 50 nucleotides in length. For NetGene2 and Neural Network Splice, the sequence analyzed is the exon length plus 100 intronic nucleotides at the exon ends. In the HSF software, if the WT score is above the threshold (65) and the score variation (between WT and Mutant) is below -10%, the mutation is considered to break the splice site. In the other case, if the WT score is below the threshold and the score variation is above +10% the mutation is considered to create a new splice site. In the MaxEnt software, if the WT score is above the threshold (3) and the score variation (between WT and Mutant) is below -30% the mutation is considered to break the splice site. In the other case, if the WT score is below the threshold and the score variation is above +30% the mutation is considered to create a new splice site. AA indicates amino acid; ASS, acceptor splice site; DSS, donor splice site; ESS, exonic splicing silencer; ESE, exonic splicing enhancer; HSF, Human Splicing Finder; MaxEnt, Maximum Entropy; NP not predicted; NT, nucleotide and; PSSM, potential splice site mutation.

Table S4. Analysis of mRNA aberrant transcript expression by next-generation sequencing

Patient code	Mutation	mRNA probes	Leukocytes		Platelets	
			% Patient Reads	% Control Reads	% Patient Reads	% Control Reads
UMP01	c.1533+1G>A	WT	28 %	100 %	100 %	100 %
		Exon 13 skipping (r.1433_1533del)	19 %	0 %	0 %	0 %
		Exon 13+14 skipping (r.1433_1729del)	45 %	0 %	0 %	0 %
		Exon 14 skipping (r.1534_1729del)	8 %	0 %	0 %	0 %
UMP02	c.3379+1G>A	WT	56 %	100 %	99 %	100 %
		Exon 25 Skipping (r.3223_3379del)	43 %	0 %	1 %	0 %
		Activation of a cryptic site at +126 nt in exon 25 (r.3349_3379del) ‡	1.4 %	0 %	0 %	0 %
UMP03	c.5664+2T>C	WT	61 %	100 %	97 %	100 %
		Exon 33 skipping (r.5621_5664del)	37 %	0 %	0 %	0 %
		Exon 33+34 skipping (r.5621_5842del) ‡	2 %	0 %	3 %	0 %
UMP08	c.546G>A	WT	98 %	99 %	NA	-
		Exon 6 skipping (r.533_657del) ‡	2.3 %	1 %	NA	-
UMP10	p.Cys370Tyr	WT	79 %	100 %	100 %	100 %
		Exon 9 skipping (r.998_1109del)	13 %	0 %	0 %	0 %
		Exon 8+9 skipping (r.875_1109del)	7 %	0 %	0 %	0 %
UMP11	p.Pro1079_Tyr1080insLeuGlnValAspProGluPro	WT	86 %	98 %	87 %	100 %
		p.Pro1079_Tyr1080insLeuGlnValAspProGluPro	14 %	2 %	13 %	0 %
UMP12	c.7082-2A>G	WT	76 %	100 %	100 %	100 %
		Activation of a cryptic site at +7 nt in exon 42 (r.7082_7088del)	24 %	0 %	0 %	0 %
UMP14	c.7437G>A	WT	58 %	99 %	NA	-
		Exon 43 skipping (r.7288_7437)	12 %	0 %	NA	-
		Activation of a cryptic splice site at +146 nt in exon 43 (r.7434_7437del)	30 %	1 %	NA	-
UMP15	c.7082-2A>G*	Exon 6 skipping (r.533_657del)	3 %	100 %	11 %	100 %
		Activation of a cryptic site at +7 nt in exon 42 (r.7082_7088del)	6 %	0 %	0 %	0 %
	c.8155+3G>C †	Exon 50 skipping (r.8116_8155del)	95 %	0 %	95 %	0 %

The values correspond to the percentage of the total reads aligned to the aberrant mRNA probes, setting as 100% the sum of reads aligned against the aberrant mRNA probes and reads aligned against the wild-type mRNA probes. NA indicates not available; and WT, wild-type. *Mutations in cis. †Mutations in trans. ‡Transcripts with low % of reads in leukocytes.

SUPPLEMENTARY FIGURES

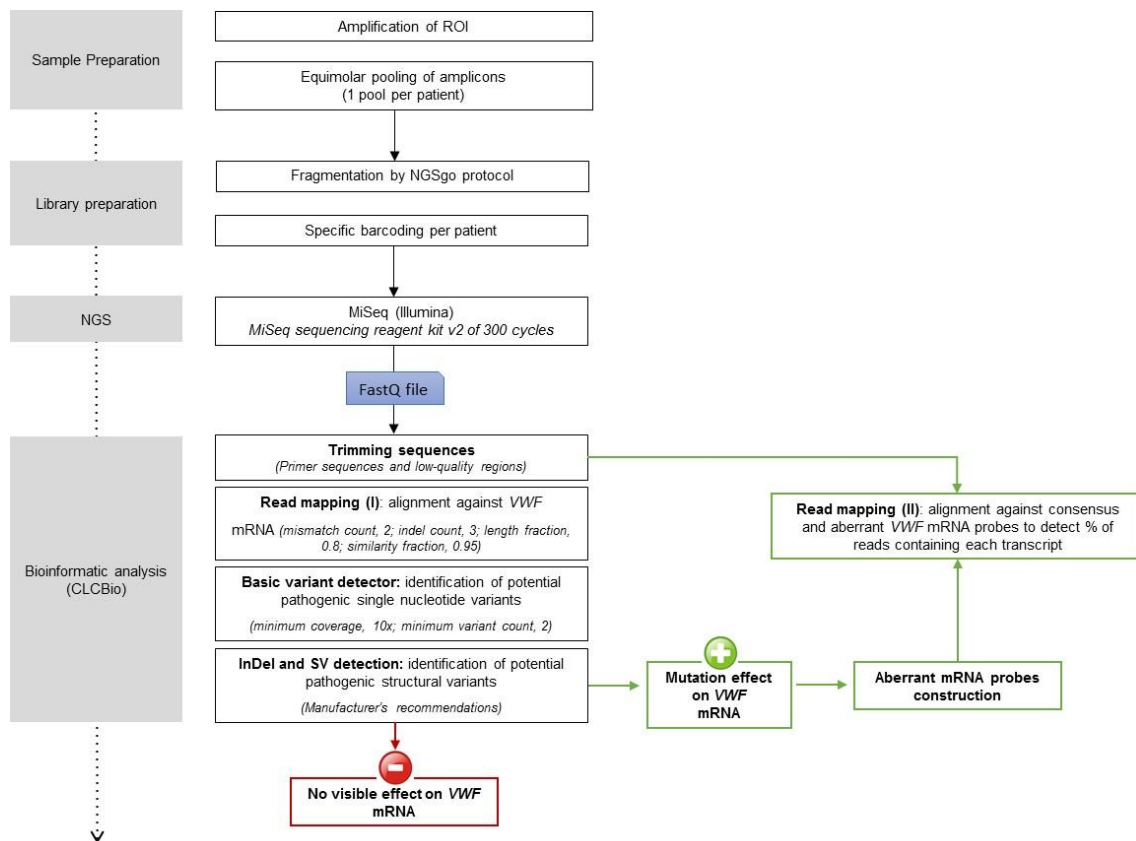


Figure S1. Flow chart used to analyze the effect of the mutation on mRNA using next-generation sequencing. ROI indicates regions of interest; NGS, next generation sequencing and; SV, structural variants.

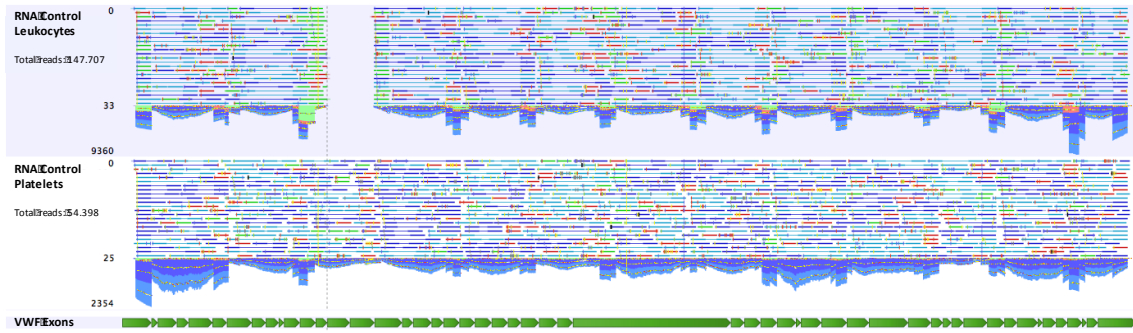


Figure S2. Schematic representation of alignment of NGS reads (from complete amplification of *VWF* mRNA from control platelets and leukocytes) to the *VWF* mRNA reference sequence. Because leukocytes show a predominant alternative splicing resulting in deletion of exon 14 (its start is shown with a discontinuous line) and exon 15, no reads were identified and mapped in this region. Except for exons 14 and 15 in leukocytes, all regions are presented with a minimum coverage of 10X in leukocytes and platelets.

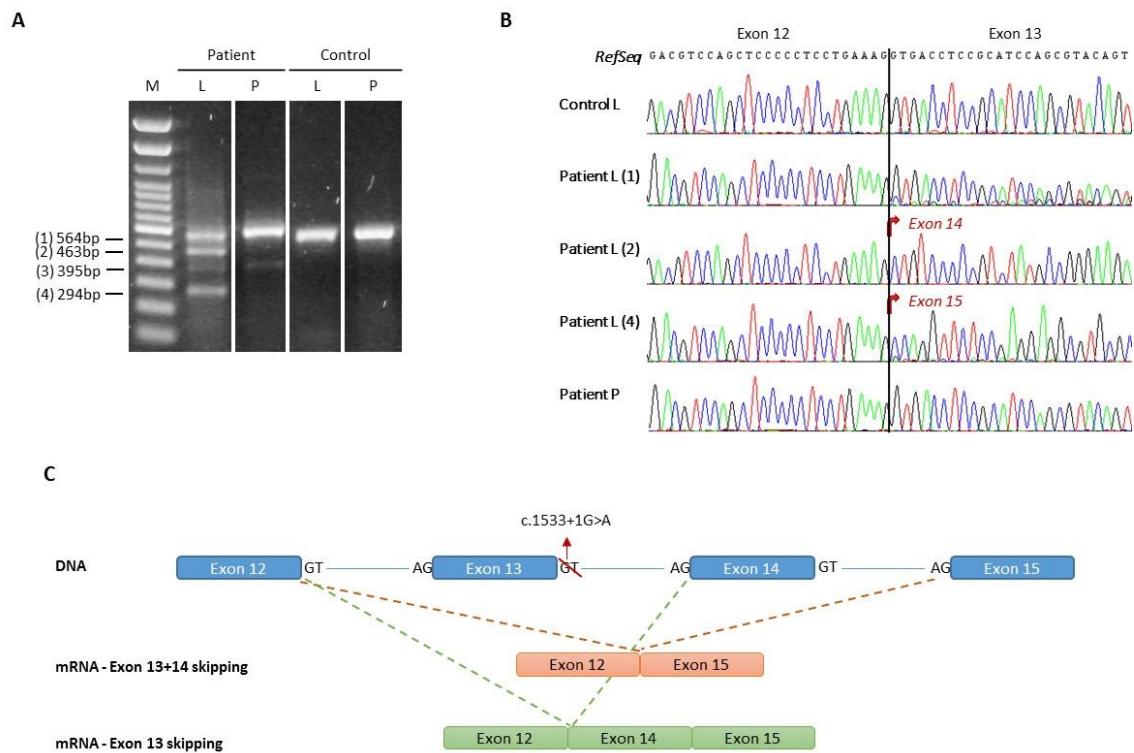


Figure S3. Analysis of the c.1533+1G>A mutation in patient UMP01. **A)** RT-PCR products amplified with primers located in exons 11 and 15 in RNA from leukocytes (L) and platelets (P) and separated on 1% agarose gel. Grouping of images from different parts of the same gel. **B)** Traditional Sanger sequencing of PCR product from patient L (1) showed the WT mRNA sequence, L (2) demonstrated exon 13 skipping and L (4) demonstrated exon 13 and 14 skipping. The L (3) band could not be purified in the agarose gel due to low concentration, thus it was not analyzed by Sanger. Platelets showed the WT mRNA sequence, indicating that the mutated allele had been degraded by NMD. **C)** Schematic representation of the mutation in genomic DNA and its effect on the *VWF* mRNA sequence. M indicates a 100-bp DNA ladder.

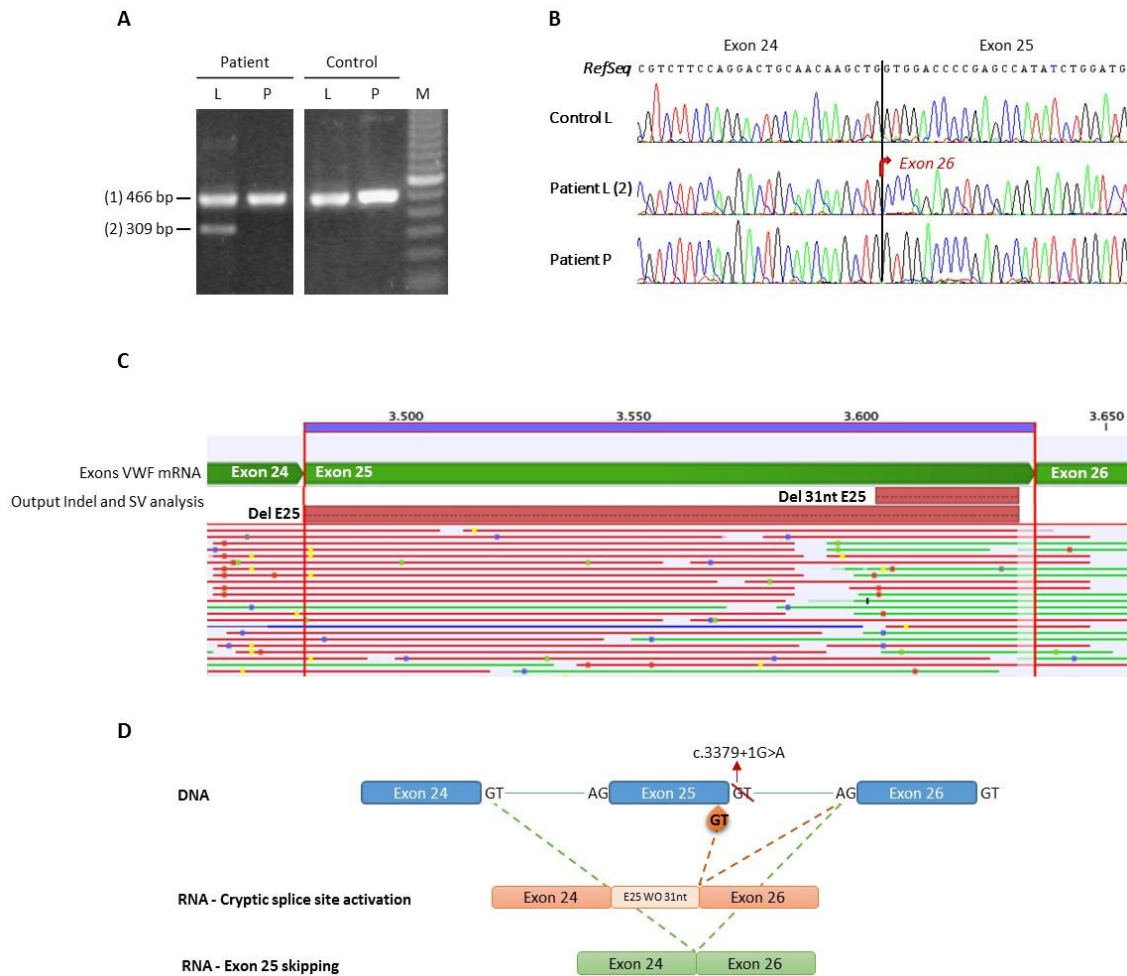


Figure S4. Analysis of the c.3379+1G>A mutation in patient UMP02. **A)** RT-PCR products amplified with primers located in exons 22 and 26 in RNA from leukocytes (L) and platelets (P) and separated on 1% agarose gel. Grouping of images from different parts of the same gel. **B)** Traditional Sanger sequencing of PCR product from patient L (2) showed exon 25 skipping. No changes were seen in the mRNA sequence in platelets, indicating that the mutated allele had been degraded by NMD. **C)** NGS of PCR products obtained from patient leukocytes identified two splicing variants: exon 25 skipping and activation of a cryptic splice site—DSS 31 nt upstream to WT-DSS—in exon 25. This last aberrant transcript was identified in a really low of transcripts. **D)** Schematic representation of the mutation in genomic DNA and its effect on the VWF mRNA sequence. M indicates 100-bp DNA ladder and; WO, without.

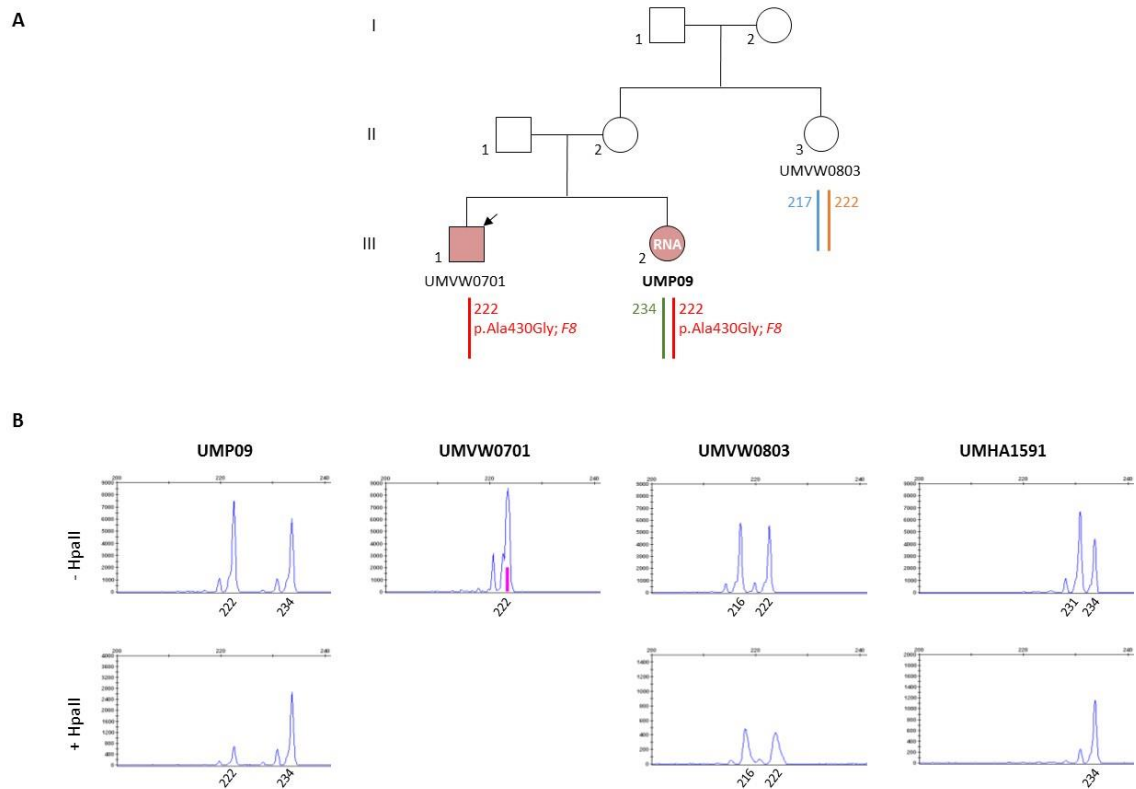


Figure S5. A) Pedigree of patient UMP09. The siblings, UMP09 and UMW0701, showed the p.Ala430Gly mutation in the F8 gene in the X chromosome with the 222 peak. The arrow shows the index case. **B)** In patient UMP09, included in this study, her maternally-derived (UMW0803) allele (222) was completely digested by the methylation-sensitive restriction enzyme Hpa II and, therefore, was not amplified by PCR. The remaining peak (234) is the paternally-derived allele representing the inactive, methylated X chromosome that resisted cleavage by Hpa II and was successfully amplified. Thus, this female patient shows complete skewing of X inactivation corresponding to the WT F8 gene. The UMHA1591 sample is a positive control for skewing of X inactivation.

REFERENCES

1. Corrales I, Ramirez L, Altisent C, Parra R, Vidal F. The study of the effect of splicing mutations in von Willebrand factor using RNA isolated from patients' platelets and leukocytes. *J Thromb Haemost.* 2011;9(4):679-688.
2. Favier R, Lavergne JM, Costa JM, et al. Unbalanced X-chromosome inactivation with a novel FVIII gene mutation resulting in severe hemophilia A in a female. *Blood.* 2000;96(13):4373-4375.